

## Design of fully reprocessable composite Non-Isocyanate Polyurethane (NIPU) foams from sustainable blends of cyclic carbonates

Federica Orabona<sup>a,b+</sup>, Federica Recupido<sup>c+</sup>, Krzysztof Polaczek<sup>c</sup>, Giuseppe Cesare Lama<sup>c</sup>, Martina Morra<sup>b</sup>, Francesco Taddeo<sup>b</sup>, Martino Di Serio<sup>b</sup>, Tapio Salmi<sup>a,b</sup>, Letizia Verdolotti<sup>c\*</sup>, Vincenzo Russo<sup>a,b\*</sup>

<sup>a</sup>*Åbo Akademi University, Johan Gadolin Process Chemistry Center (PCC), Laboratory of Industrial Chemistry and Reaction Engineering (TKR), Henriksgatan 2, FI-20500, Turku/Åbo, Finland.*

<sup>b</sup>*University of Naples Federico II, Chemical Sciences Department, Via Cintia 26, 80126 Naples, Italy.*

<sup>c</sup>*National Research Council, Institute for Polymers, Composites and Biomaterials, 80055 Portici, Naples, Italy.*

+ *These authors equally contributed to this work.*

\**Corresponding authors: Letizia Verdolotti; [letizia.verdolotti@cnr.it](mailto:letizia.verdolotti@cnr.it) and Vincenzo Russo [v.russo@unina.it](mailto:v.russo@unina.it)*

### Supporting information

Section S1	Experimental set-up to synthesize CSBO
Section S2	Characterization of ESBO
Section S3	Chemical and thermal characterization of the precursors
Section S4	FTIR analysis of NIPU foams
Section S5	DSC thermograms of NIPU foams
Section S6	FTIR and DSC thermogram of the NIPU film

## S1 Experimental conditions used in the synthesis of CSBO

ESBO was employed as the starting material for the cycloaddition of CO<sub>2</sub> to synthesize the respective cyclic carbonate i.e., CSBO. The experiments were performed in a Parr reactor (**Figure S1**).

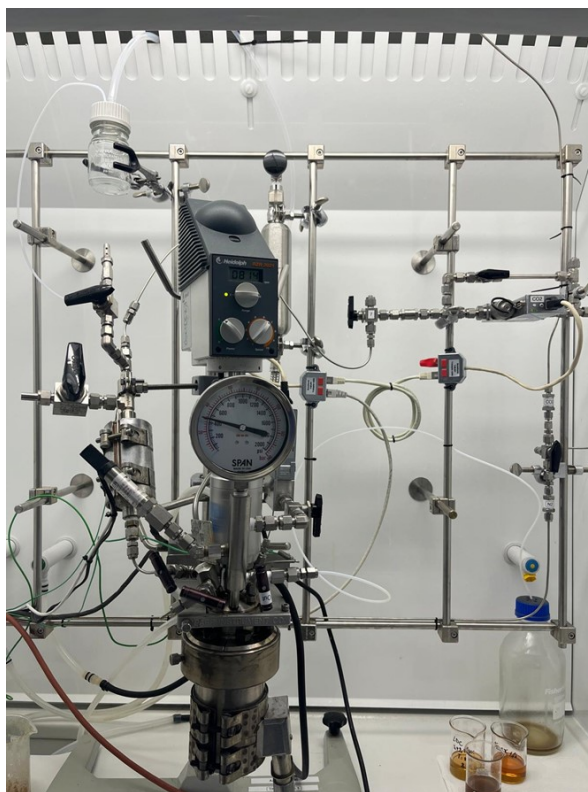


**Figure S1.** Experimental set-up for the carbonation experiments.

The ESBO conversion and the yield of the CSBO and keto-byproduct were measured by quantitative <sup>1</sup>H-NMR 500 MHz employing CDCl<sub>3</sub> as a solvent. The ESBO conversion was calculated according to equation 1, where  $R_{ESBO}$  is the ratio of the peak areas in the region 2.9-3.15 ppm normalized by the number of hydrogen atoms with respect to a reference peak. Specifically, the -CH- hydrogen of the second carbon in the glycerol backbone at 5.27 ppm was employed as a reference <sup>1</sup>. The CSBO and keto-byproduct yields were calculated according to Equation 2 and 3, respectively. The peaks at 4.2-5.1 ppm normalized by the number of hydrogens were selected to obtain  $R_{CSBO}$ , while the peaks at 2.4 ppm were considered to calculate the keto-byproduct ratio  $R_{KetoBP}$ . **Figure S2** illustrates the conversion and yields respect to the reaction time.

$$Conversion_{ESBO} = \frac{R_{ESBO,t_0} - R_{ESBO,t}}{R_{ESBO,t_0}} \cdot 100 \quad (1)$$

$$Yield_{CSBO} = \frac{R_{CSBO,t}}{R_{ESBO,t_0}} \cdot 100 \quad (2)$$

$$Yield_{KetoBP} = \frac{R_{KetoBP,t}}{R_{ESBO,t_0}} \cdot 100 \quad (3)$$

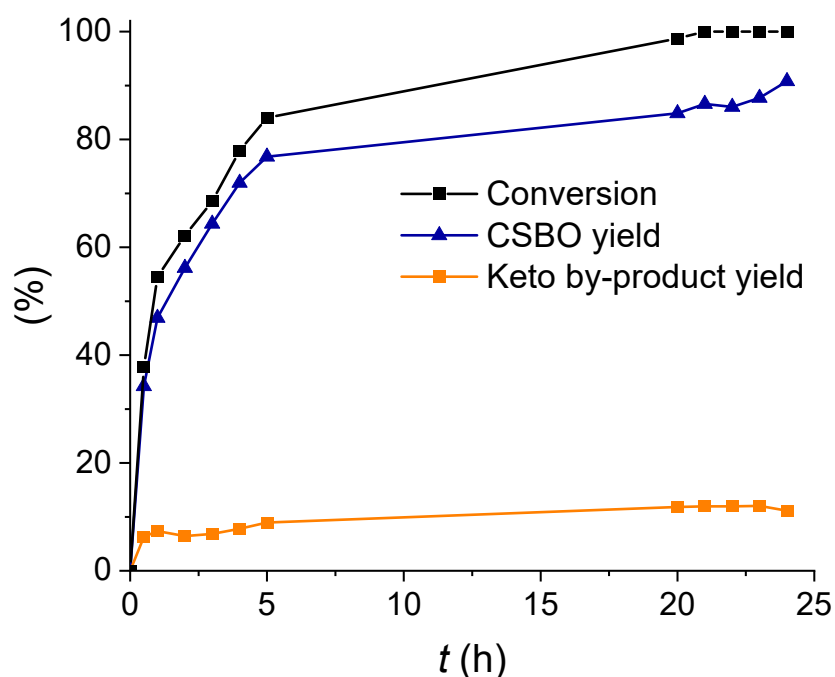


**Figure S2.** ESBO conversion, CSBO, and keto-byproduct yields over time of reaction.

Considering the CSBO yield, its average functionality  $\bar{f}_{CSBO}$  was calculated according to equation 4 and resulted to be 3.7. The desired weight of CSBO is obtained according to Equation 5.

$$\bar{f}_{CSBO} = \sum (f \cdot w / w \cdot 3) \cdot yield_{CSBO} = 3.7 \quad (4)$$

$$w_{CSBO} = \frac{n_{CSBO} MW_{CSBO}}{\bar{f}_{CSBO}} \quad (5)$$

## S2. Characterization of epoxidized soybean oil (ESBO)

The ESBO double bond content was evaluated via titration following the standard method ASTM D5554-15. The concentration of the ESBO epoxy groups was 4.43 mol/L, whereas the iodine value 6.58 g<sub>Iodine</sub>/100 g<sub>oil</sub>, in agreement with the supplier. Generally, the iodine value of soybean oil is approximately 130 g<sub>Iodine</sub>/100 g<sub>oil</sub><sup>2</sup>, therefore, the starting material can be regarded as highly pure.

The fatty acid composition was determined through Gas Chromatography-Mass Spectroscopy (GC-MS), after proper trans-esterification of the oil according to the procedure reported by Cai et al.<sup>3</sup>. The National Institute of Standards and Technology (NIST) library was employed as the main database for the mass spectra. The fatty acid composition of the ESBO in w/w% determined by GC-MS is shown in Table S1.

**Table S1.** Fatty acid composition results obtained from GC-MS analysis.

<b>Fatty acid methyl ester</b>	<b>Functionality, <i>f</i></b>	<b>w/w%</b>
Palmitic acid methyl ester (C16:0)	0	16.1
stearic acid methyl ester (C18:0)	0	6.0
oleic acid methyl ester (C18:1)	1	19.9
linoleic acid methyl ester (C18:2)	2	48.4
linolenic acid methyl ester (C18:3)	3	7.0
Eicosanoic acid methyl ester (C20:0)	0	1.7
Docosanoic acid methyl ester (C22:0)	0	1.0

### S3. Characterization of the foam precursors

#### S.3.1 Thermal characterization

Temperature at 5 % weight loss ( $T_{5\%}$ ), the maximum temperature at first degradation step ( $T_{\max 1}$ ), the maximum temperature at second degradation step ( $T_{\max 2}$ ) and the char at 600°C of the selected precursors are indicated in **Table S2**.

**Table S2.** Temperature at 5 % weight loss ( $T_{5\%}$ ), the maximum temperature at first degradation step ( $T_{\max 1}$ ) and the char at 600°C of the selected precursors.

Precursor	$T_{d5\%}$ (°C)	$T_{d\max 1}$ (°C)	$T_{d\max 2}$ (°C)	Char at 600°C (%)
CSBO	65.8	95.3	409.1	0.4
BCC	257.6	-	308.2	0.4
DODT	122.2	188.4	-	negligible

The synthesized CSBO presented two degradation stages. The first one is mainly associated with solvent evaporation ( $T_{\max 1}$ ), while  $T_{\max 2}$  refers to the decomposition of fatty acid chains as reported by Lee et al., 2024<sup>4</sup>. For the case of BCC, the degradation temperature ( $T_{d5\%}$ ) was achieved at 257.6°C, whereas, the maximum degradation temperature was around 300°C (related to the complete decomposition of carbonyl groups and formation of acetaldehyde)<sup>5</sup>, resulting in lower thermal stability compared to CSBO. DODT presented a maximum temperature of 188.4°C.

#### S.3.2 Chemical characterization

The FTIR spectra of the precursors are shown in **Figure S3**. The bis-cyclic carbonate (BCC) exhibited characteristic absorption bands corresponding to asymmetric and symmetric stretching vibrations of C–H groups ( $\nu$ -CH<sub>2</sub> and  $\nu$ -CH<sub>3</sub>) at 2930 and 2850 cm<sup>-1</sup>, respectively. A strong absorption peak at 1780 cm<sup>-1</sup> was attributed to the stretching vibration of the carbonyl group (C=O)<sup>6</sup>. Additionally, a broad shoulder observed in the 1000–1200 cm<sup>-1</sup> range is associated with C–O–C (ether) stretching vibrations, with a prominent band centered at approximately 1100 cm<sup>-1</sup>.

The FTIR spectrum of 1,4-butanediamine (BDA) displayed two prominent features. The first was a double peak in the 3400–3200 cm<sup>-1</sup> region, corresponding to the N–H stretching vibrations of aliphatic primary amine groups. The second feature, spanning 3200–2800 cm<sup>-1</sup>, was attributed to C–H stretching vibrations of methyl groups.

In the case of 2,2'-dithiodiethanethiol (DODT), a distinct peak appeared at ~2500 cm<sup>-1</sup>, characteristic of the S–H stretching vibration. Additional bands in the 3000–2800 cm<sup>-1</sup> region corresponded to C–H stretching modes. A clear absorption at 1150 cm<sup>-1</sup> was associated with C–O–C stretching, and a peak at 670 cm<sup>-1</sup> was assigned to C–S vibrations, consistent with previous literature<sup>7</sup>.

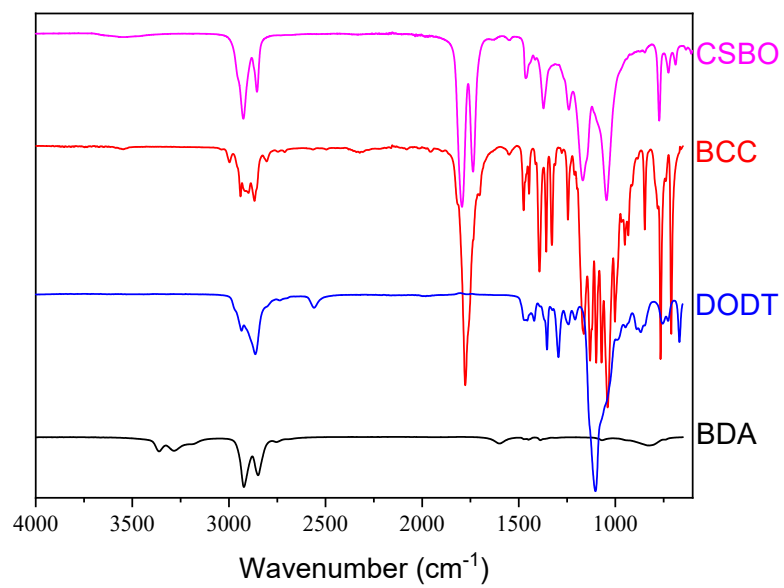


**Figure S3.** FTIR spectra of NIPU foam precursors in the wavenumber range of 4000-600 cm<sup>-1</sup>.

#### S4. FTIR spectra of NIPU foams

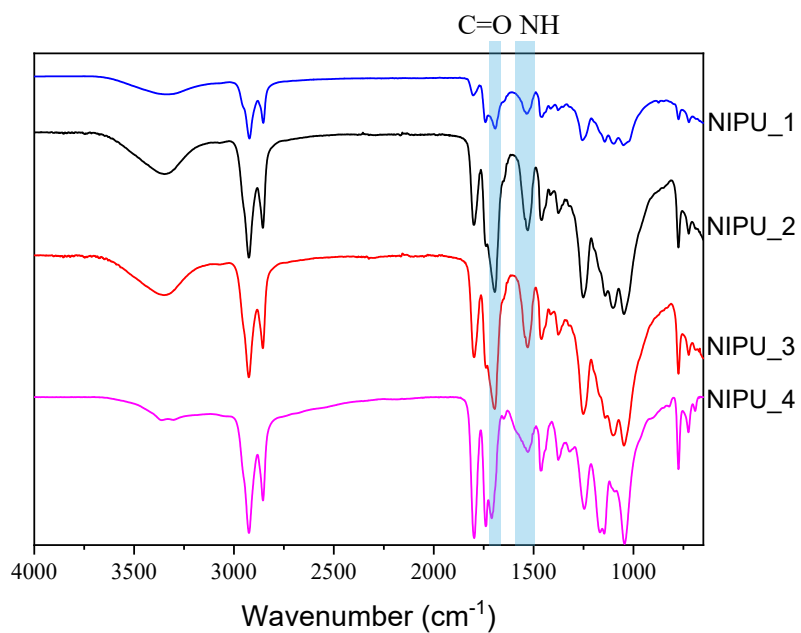


Figure S4. FTIR spectra of NIPU\_1-NIPU\_4 foams in the wavenumber range of 4000-600  $\text{cm}^{-1}$ .

#### S5. DSC curves of the NIPU foams

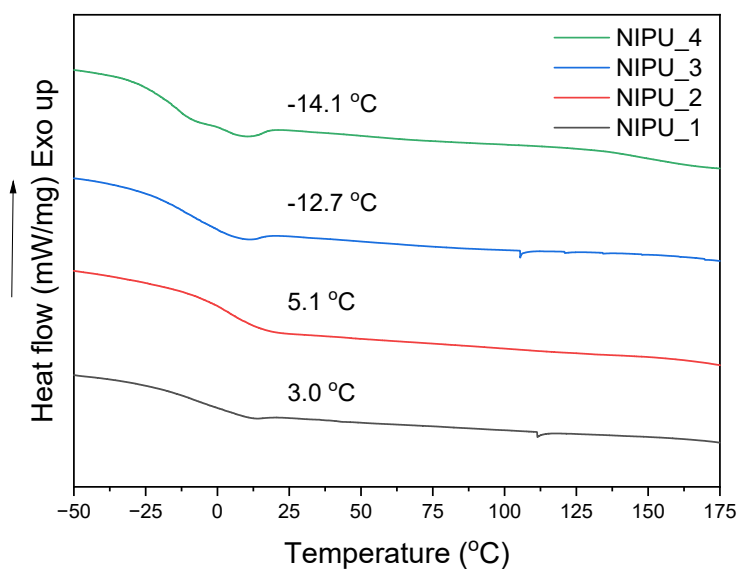


Figure S5. DSC thermograms of the selected NIPU foams.

## S6. FTIR spectra and DSC curve of the NIPU foams and film

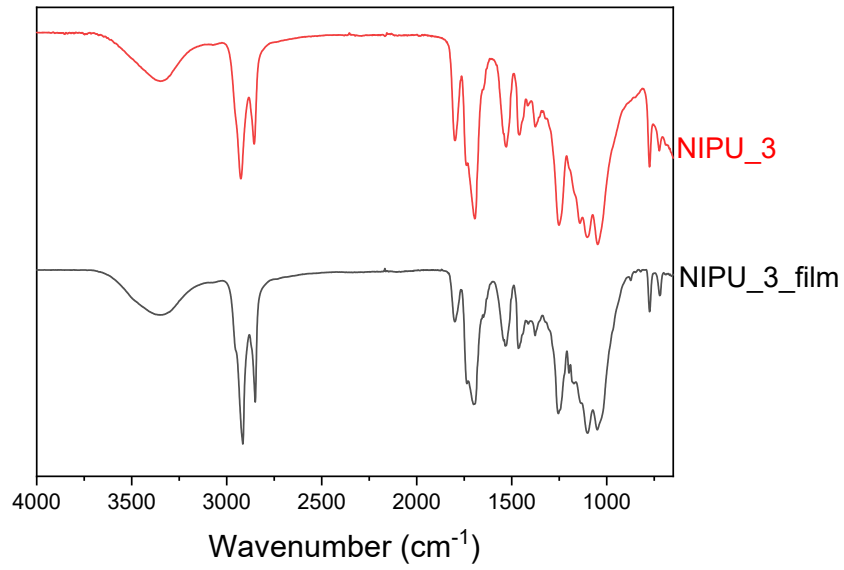


Figure S6. FTIR spectra of NIPU\_3 and NIPU\_3\_film in the wavenumber range of 4000-600 cm<sup>-1</sup>.

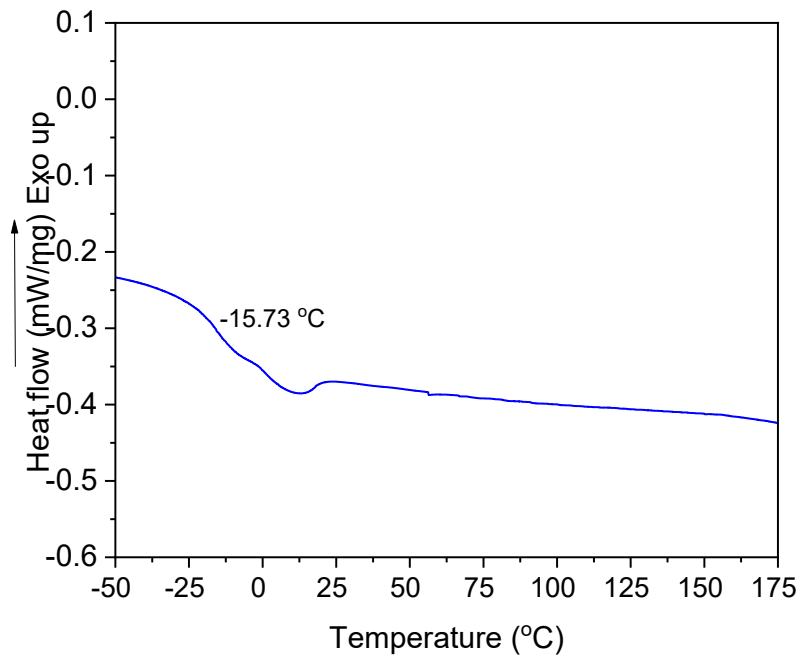


Figure S7. DSC thermogram of NIPU\_3\_film.

## References

- [1] T. Cogliano, R. Turco, V. Russo, M Di Serio, R. Tesser, *Ind. Crops Prod.* 2022, **186**,115258, <https://doi.org/10.1016/j.indcrop.2022.115258>
- [2] N.K. Kyriakidis, T. Katsiloulis, *J. American Oil Chem. Soc.* 2000, **77(12)**, 1235-1238, <https://doi.org/10.1007/s11746-000-0193-3>
- [3] X. Chai, M. Matos, S. *Ind. Eng. Chem. Res.* 2019, **58(4)**, 1548–1560, <https://doi.org/10.1021/acs.iecr.8b05510>
- [4] G. Ram Lee, E. Jong Lee, H. Sun Shin, J. Kim, I. Kim, S. Chun Hong, *Polymers* 2024, **16(8)** 1171, <https://doi.org/10.3390/polym16081171>
- [5] K. Blázquez, J. Datta, A. Cichoracka, *Polym Int.* 2019, **68**, 1968–1979, <https://doi.org/10.1002/pi.5908>
- [6] K. Blázquez, H. Beneš, Z. Walterová, S. Abbrent, A. Eceiza, T. Calvo-Correas, J. Datta, *Polym. Chem.* 2021, **12**,1643, DOI: 10.1039/d0py01576h
- [7] E.Q. Rosenthal, J.E. Puskas, C. Wesdemiotis, *Biomacromolecules* 2012, **13**, 154-164, [dx.doi.org/10.1021/bm201395t](https://doi.org/10.1021/bm201395t)